Available online at www.sciencedirect.com
ScienceDirect
Dyes and Pigments 76 (2008) 492–498
DYES and PIGMENTS
www.elsevier.com/locate/dyepig

Synthesis and 0.88 μm near-infrared electroluminescence properties of a soluble chloroindium phthalocyanine

Shukun Yu [a], Chunyu Ma [b], Chuanhui Cheng [a], Xu Wang [c], Dongmei Ji [a], Zhaoqi Fan [a], Daocheng Xia [b], Wei He [b], Yuchun Chang [a], Guotong Du [a,b,*]

[a] *State Key Laboratory of Integrated Optoelectronics, College of Electronic Science and Engineering, Jilin University, Qianjin Street 2699, Changchun 130012, China*
[b] *State Key Laboratory of Materials Modification by Laser, Ion and Electron Beams, Department of Physics, Dalian University of Technology, 116024 Dalian, China*
[c] *Key Laboratory for Supramolecular Structure and Materials, College of Chemistry, Jilin University, 130012 Changchun, China*

Received 29 September 2006; received in revised form 11 October 2006; accepted 14 October 2006
Available online 20 November 2006

Abstract

A chloroindium phthalocyanine bearing phenoxyl substituents was synthesized and characterized by MS, ^{1}H NMR and elemental analysis, which were consistent with the proposed structure; UV–vis absorption and photoluminescence (PL) spectra were also investigated. Near-infrared (NIR) organic light-emitting devices (OLEDs) were fabricated employing tris-(8-hydroxyquinoline) aluminum (Alq_3) and poly(vinylcarbazole) (PVK) which had been doped with chloroindium phthalocyanine. Room-temperature electroluminescence (EL) was observed near 0.88 μm due to transitions from the first excited singlet state to the ground state (S_1–S_0). As phthalocyanine possesses excellent solubility in common organic solvents, the light-emitting layer can be prepared by spin coating to simplify the fabrication process and so lower the manufacturing costs. The emission processes of this chloroindium phthalocyanine in the doped devices are discussed.

Keywords: Phthalocyanine; Dye synthesis; Organic light-emitting diodes; Near-infrared; Electroluminescence

1. Introduction

Since the initial discovery of OLEDs in 1987 [1], the devices have attracted extensive research from both academic and technological viewpoints for full-color flat-panel displays with high brightness and rapid response. Majority of the research has focused on devices that emit light in the wavelength range from the blue-violet to visible light. Recently, near-infrared (NIR) OLEDs have received attention due to their potential application in optical communications [2]. However, the emission efficiency of NIR OLEDs is generally low because of near-field deactivation by the host associated with coupling of the optically excited state to the vibrations of the organic molecule or polymer [3]. The materials used in NIR OLEDs have been limited in number, most of them being organic complexes containing trivalent rare earth ions, such as Er^{3+}, Nd^{3+}, Tm^{3+} and Yb^{3+} [3–6]; only a few organic materials [7] containing no rare earth ions display electroluminescence in the NIR region.

Phthalocyanine (Pc) is a prominent class of organic molecular material which characteristically possesses high chemical and thermal stability. In particular, phthalocyanines and their derivatives can be used remarkably as functional materials and enjoy applications in a wide range of high technical fields such as nonlinear optics, liquid crystals, Langmuir–Blodgett films, photovoltaic cells, chemical sensors, laser recording materials, organic field effect transistors and even biomedical applications [8–11]. Recently, several Pcs have been used as the hole-transport layer [12], the contact modification layer and

* Corresponding author. State Key Laboratory of Integrated Optoelectronics, College of Electronic Science and Engineering, Jilin University, Qianjin Street 2699, Changchun 130012, China. Fax: +86 431 5168270.
E-mail address: yushukun@email.jlu.edu.cn (G. Du).

0143-7208/$ - see front matter © 2006 Elsevier Ltd. All rights reserved.
doi:10.1016/j.dyepig.2006.10.009

the light-emitting layer [13] in OLEDs. We have reported a NIR OLED emitting near 1.1 μm based on 4, 4′-*N*,*N*′-dicarbazole-biphenyl (CBP) doped with copper phthalocyanine (CuPc) [14]. OLEDs based on a mixture of host polymer and small guest molecules have attracted much attention as a promising inexpensive technology for large-area and flexible devices because the light-emitting layer of OLEDs can be prepared using a wet process, such as spin coating or ink-jet printing [5,6]. However, as with most small molecular size materials, Pcs are insoluble and difficult to process. Efforts to solubilize these materials have included the incorporation of side chains, such as the addition of alkyl groups, aryl groups or heterocyclic groups [15,16].

In this paper, a soluble chloroindium 1,8(11),15(18),22(25)-tetra-(*p-tert*-butylphenoxy) phthalocyanine (ClInPc) was synthesized and characterized by MS, ^{1}H NMR, elemental analysis, UV–vis and PL. For the purpose of testing its EL properties, single-layer OLEDs with the structure ITO/ClInPc/Al were prepared; however, these devices did not show any measurable EL and so the EL properties of the new compound were also studied in ITO/NPB/Alq_3:ClInPc/Alq_3/Al devices with different ClInPc concentrations. Room-temperature EL was observed near 0.88 μm that effectively covered the first optical communication window near 0.85 μm. OLEDs were fabricated employing this ClInPc dispersed in PVK as the emitting layer by spin coating; 0.88 μm NIR EL was observed for these ITO/PVK:ClInPc/BCP/Alq_3/Al devices.

2. Experimental

2.1. Materials and equipments

Solvents were purified according to standard procedures. All other materials were obtained commercially and used without further purification.

MS spectra were obtained using an LDI-1700-TOF mass spectrometer (Linear Scientific Inc., USA). High-resolution ^{1}H NMR spectra were recorded on a Bruker AV 500 spectrometer. Elemental analysis was performed on a Flash A1112 Elemental Analyzer (ThermoQuest, Italy). UV–vis spectra were taken on a UV-3100 UV–VIS–NIR Recording Spectrophotometer (Shimadzu, Japan). Current (I) versus voltage (V) measurements were obtained using a Keithley 2400 current–voltage source. NIR PL spectra were obtained on a PL9000 Photoluminescence System (Bio-Rad Micromeasurements Ltd, UK); the NIR EL signals were focused into a monochromator and detected with a liquid-nitrogen-cooled Ge detector, using standard lock-in techniques.

2.2. Synthesis of chloroindium 1,8(11),15(18),22(25)-tetra-(p-tert-butylphenoxy) phthalocyanine

Treatment of 3-nitrophthalonitrile (**1**, 1.73 g, 10 mmol) and *p-tert*-butylphenol (**2**, 1.50 g, 10 mmol) in the presence of $LiOH\cdot H_2O$ (1.05 g, 25 mmol) and anhydrous DMSO (30 mL) at room temperature for 48 h afforded the expected 3-(*p-tert*-butylphenoxy) phthalonitrile (**3**) (Fig. 1) in good yield (78%), which was purified by column chromatography on silica gel with petroleum ether–diethyl ether as eluent [17,18]. 3-(*p-tert*-Butylphenoxy) phthalonitrile (**3**, 1.16 g, 4.2 mmol) and $InCl_3\cdot 4H_2O$ (0.308 g, 1.05 mmol) were added to quinoline (8 mL) with stirring in the presence of DBU, which was heated at 200 °C under N_2 for 12 h (Fig. 1). After cooling to room temperature the reaction mixture was poured into 100 mL of a mixture of methanol and deionized water (4:1) and the precipitate was collected and extracted with anhydrous methanol in a Soxhlet extractor. The solvent was removed under reduced pressure and the ensuing solid was purified using column chromatography on silica gel with diethyl ether–petroleum ether (1:3) as the eluent. After evaporation of the eluent, the blue-green ClInPc (**4**) was obtained in good yield (49%, 645 mg) [17,18] which was purified three times by vacuum sublimation using a three-zone furnace before device fabrication. ^{1}H NMR ($CDCl_3$): $\delta = 7.376$–7.503 (m, 12H, ArH), 7.124–7.260 (m, 16H, ArH), 1.368–1.437

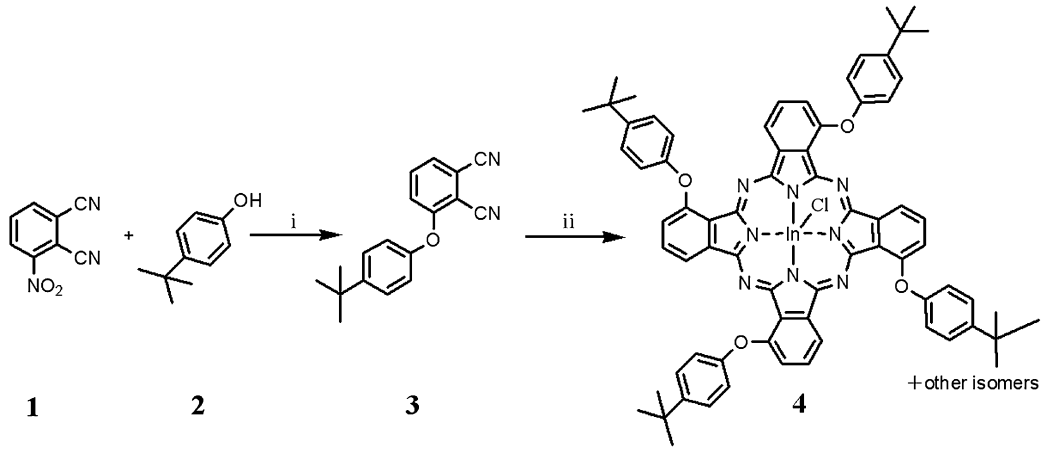

i : DMSO, $LiOH\cdot H_2O$, 30℃, 78% ; ii : Quinoline, DBU, $InCl_3\cdot 4H_2O$, 49%

Fig. 1. The synthetic route of a soluble ClInPc.

(m, 36H, $12CH_3$). MS: $m/z = 1255.2$ $[M + H^+]$ (calcd. 1255.4). Anal. calcd. for $C_{72}H_{64}N_8O_4ClIn$: C, 68.87; H, 5.14; N, 8.92. Found: C, 68.65; H, 5.17; N, 8.86.

2.3. Fabrication of EL devices

Indium tin oxide (ITO) coated glass substrates with a sheet resistance of ~20 Ω/□ and transmittance of ~90% near 0.88 μm were sequentially cleaned with acetone, ethanol and deionized water for 15 min in an ultrasonic cleaning bath. Single-layer OLEDs were fabricated by vacuum evaporating ClInPc onto the pre-cleaned substrates, varying the ClInPc layer thickness from 30 to 100 nm. OLEDs with the structure: ITO/NPB/Alq_3:ClInPc/Alq_3/Al were fabricated by successive vacuum ($<1 \times 10^{-3}$ Pa) deposition of the organic materials onto the clean substrates at a deposition rate of 20–40 Å min^{-1}. A 30-nm-thick film of *N*,*N*′-di-1-naphthyl-*N*,*N*′-diphenylbenzidine (NPB) served as the hole-transport layer (HTL). A 30-nm-thick ClInPc-doped Alq_3 (0–75 wt%) layer was deposited as the light-emitting layer by simultaneous evaporation from two separate sources. After that, another 10-nm-thick Alq_3 was used to transport and inject electrons. To fabricate the ITO/PVK:ClInPc/BCP/Alq_3/Al devices, a 40-nm-thick ClInPc-doped PVK (0–80 wt%) layer was spin-coated onto the ITO surface at 3000 rpm from a chloroform solution (6 mg/mL) and subsequently cured in a vacuum oven at 120 °C for 2 h. The thickness of the spin-coated film was verified using an ellipsometer. An 18-nm-thick layer of 2,9-dimethyl-4,7diphenyl-1,10-phenanthroline (BCP) was deposited as the hole-blocking layer and a 15-nm-thick Alq_3 layer was used to transport and inject electrons. Finally a shadow mask comprising 3 mm × 3 mm openings was used to define the 120-nm-thick Al cathode for all three types of device. The chemical structures of Alq_3, PVK, NPB, BCP and the device configurations used in this work are shown in Fig. 2.

3. Results and discussion

3.1. Synthesis and characterization

A commonly used synthetic route to realise soluble tetra-substituted Pcs involves the aromatic nucleophilic substitution reaction between 3-nitrophthalonitrile or 4-nitrophthalonitrile and a suitable oxygen, nitrogen or sulfur nucleophile followed by cyclotetramerization of the resultant phthalonitrile derivatives, e.g. 4-(cumylphenoxy) phthalonitrile [19] and 4-(neopentoxy) phthalonitrile [20]. This particular approach was employed in the synthesis of the soluble ClInPc and its precursor in this work.

In DMSO, the anion of *p*-*tert*-butylphenol displaced the nitro group of 3-nitrophthalonitrile in the presence of $LiOH \cdot H_2O$ as the alkali to generate the corresponding phthalonitrile derivative in good yield. ClInPc was characterized by elemental analysis and spectroscopic methods including ^1H NMR and TOF-MS, which were consistent with the proposed structure. The ^1H NMR spectra (500 MHz, $CDCl_3$) of the precursor and ClInPc did not display signals of impurities. The preparation of metal Pcs by cyclotetramerisation of phthalonitrile derivatives, catalysed by DBU, in quinoline is preferable due to its easier purification and higher yield. ClInPc has excellent solubility in common organic solvents, such as $CHCl_3$, CH_2Cl_2, THF and benzene, which is advantageous in the establishment of molecular order systems and helpful in the investigation of physical and chemical properties of molecular order systems.

3.2. Optical properties

Fig. 3 shows the UV–vis absorption spectra of ClInPc in chloroform solution and in vacuum sublimed films on quartz substrates. The UV–vis absorption spectra exhibited the characteristic B- and Q-bands of Pcs, which can be assigned to be

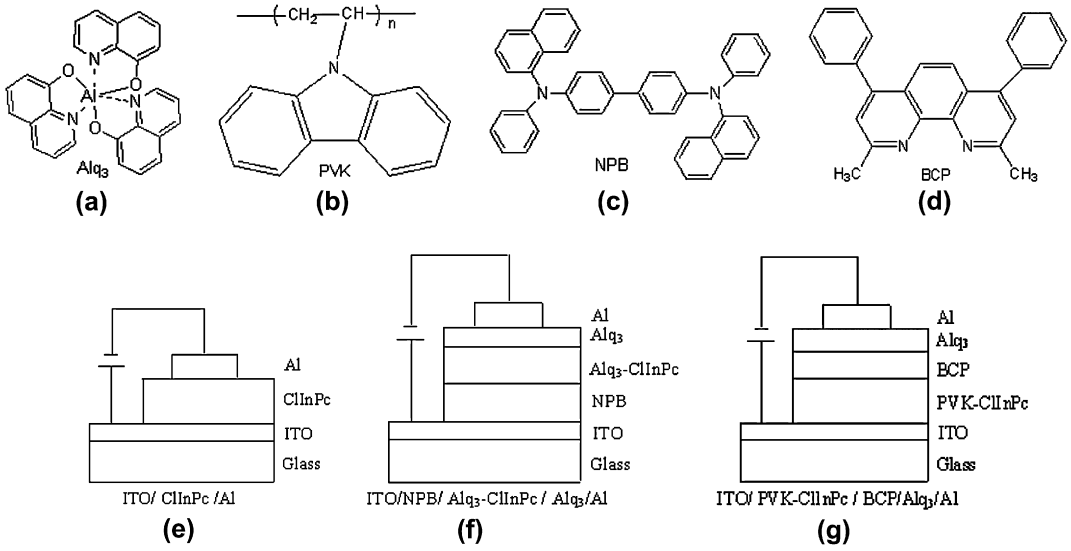

Fig. 2. The chemical structures of other materials used in OLEDs: (a) Alq_3, (b) PVK, (c) NPB and (d) BCP. The device configurations of OLEDs used in this work: (e) ITO/ClInPc/Al, (f) ITO/NPB/Alq_3:ClInPc/Alq_3/Al and (g) ITO/PVK:ClInPc/BCP/Alq_3/Al.

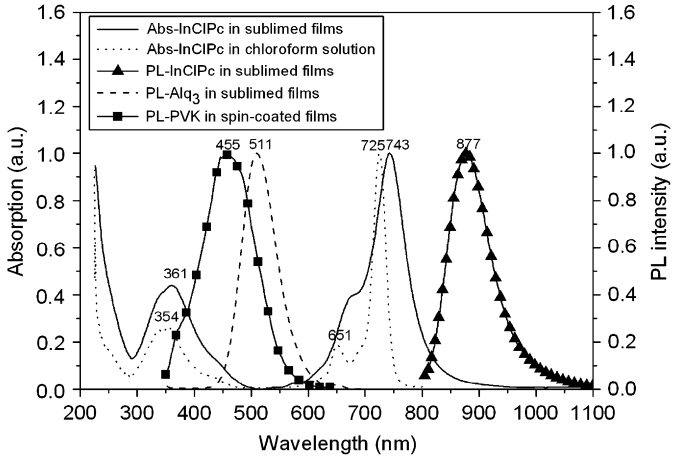

Fig. 3. Left: Normalized UV–vis absorption spectrum of ClInPc in chloroform solution and in vacuum sublimed films; Right: Normalized PL spectra of ClInPc films (excited at 488 nm), Alq_3 films and PVK films (excited at 325 nm).

$\pi-\pi^*$ transition of the conjugated system. The absorption peaks at 354 nm in chloroform solution and 361 nm in the sublimed films corresponded to the B band, whereas those at 725 nm in chloroform solution and 743 nm in the sublimed films correspond to the Q band.

A small band appearing at 651 nm in chloroform solution cannot be attributed to the dimer because no broadening of the Q band [21] was observed with increasing concentration increasing upto 10^{-4} mol/L; hence, the small band can be attributed to electronic vibration. Aggregation of Pcs in solution is easily detected using optical absorption studies in terms of a decrease in the maximum extinction coefficient and a blue shift of the Q band [15]. When the UV–vis spectrum of ClInPc was measured in $CHCl_3$ at a concentration as high as 1.2×10^{-4} M, the observed band shape changed slightly and the peak corresponding to the monomer at 725 nm was still evident. Thus, the absorption of ClInPc in solution was governed by monomer-absorption. Similar absorption spectra have been observed in vacuum sublimed films of ClInPc [22]. The absorption spectrum of the sublimed film was broader, as expected, and included a wing beyond 800 nm, but the position of the Q band was only slightly shifted in the sublimed films compared with the chloroform solution. This was consistent with the relatively weak aggregation of this ClInPc.

The UV–vis spectra show the weakly aggregative nature of ClInPc, which may arise from steric hinderance of the bulky peripheral groups [16] and the axial substituents [22–24] hindering $\pi-\pi^*$ interaction among the ClInPc molecules. This weak aggregation behaviour could have important advantages not only for studying intermolecular processes in the compound but also for the application of this compound in photodynamic therapy.

Fig. 3 also shows the PL spectrum of ClInPc vacuum sublimed film on quartz substrate excited using a 488 nm line from an Ar^+ laser. The sublimed films emitted a somewhat broadened peak centered at 877 nm, which can be assumed to be molecular fluorescence due to transitions from the first excited singlet state to the ground state (S_1-S_0). In comparison to the absorption spectrum of sublimed films, the emission spectrum was shifted by approximately 130 nm towards the long wavelength side.

3.3. EL properties

To investigate the EL properties of ClInPc, single-layer device with the structure: ITO/ClInPc/Al and multi-layer devices with the structures: ITO/NPB/Alq_3:ClInPc/Alq_3/Al and ITO/PVK:ClInPc/BCP/Alq_3/Al were fabricated as described earlier.

The single-layer device consisting of ClInPc between ITO and Al electrodes did not show any measurable EL, which may be due to unbalanced charge injection and unbalanced charge transport in the ClInPc layer. A three-layer doped structure: ITO/NPB/Alq_3:ClInPc/Alq_3/Al was used to raise the emission level. Fig. 4(a) shows the NIR EL spectra of the devices with different doping concentrations of ClInPc in Alq_3 at 10 mA at room temperature. The emission near 0.88 μm coincided with the PL spectrum in the sublimed films of ClInPc

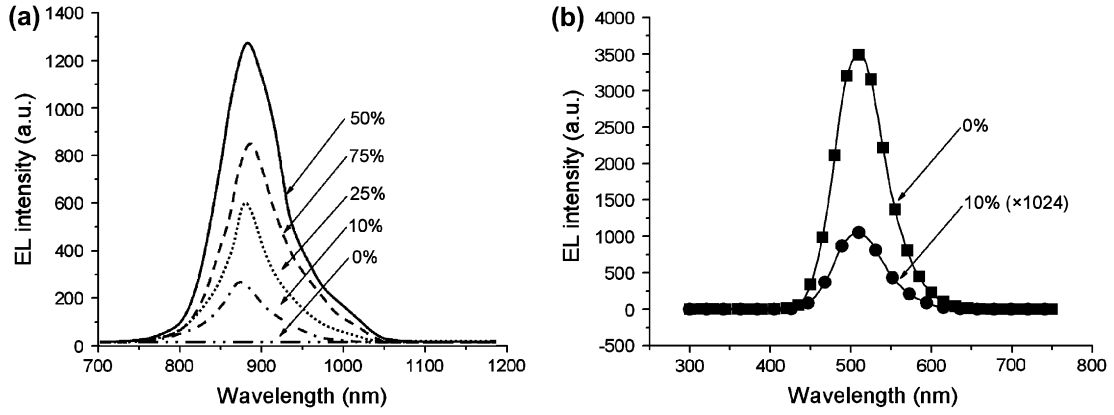

Fig. 4. (a) The NIR EL spectra of devices with the structure of ITO/NPB/Alq_3:ClInPc/Alq_3/Al with different ClInPc doping concentrations. (b) The UV–vis EL spectra of devices with the structure of ITO/NPB/Alq_3:ClInPc/Alq_3/Al with different ClInPc doping concentrations. The sensitivity of 10% doped devices is 1024 times that of undoped devices.

(Fig. 3). When the concentration of ClInPc was higher than 50% by mass, the intensity of the NIR emission decreased with increasing dope concentration. This may be due to fluorescence quenching becoming significant at high concentration. The optimum concentration was 50% by mass, which implied a weak, aggregation-induced quenching of ClInPc in the solid films because of restrained face-to-face intermolecular coupling owing to the presence of the four bulky phenoxyl substituents and axial substitution. It is well known that functional groups hamper aggregation and increase the quantum-efficiency for EL in the case of small organic molecules as for conjugated polymers [25,26]. Previously published work [16] supports the results found herein, in which Pcs bearing extremely bulky polyoxyethylene substituents display strong red fluorescence in the absence of aggregation-induced quenching.

Fig. 4(b) shows the UV–vis EL spectra of devices with the structure: ITO/NPB/Alq_3:ClInPc/Alq_3/Al in which different doping concentrations of ClInPc in Alq_3 were used, at 10 mA at room temperature. The green emission of the doped devices and undoped devices near 510 nm came from Alq_3. There existed no emission of NPB near 455 nm in these devices. The Alq_3 emission decreased in intensity with increasing dope concentration and the emission became difficult to measure at a dope level >10% by mass.

There are two possible ways for electrically exciting the guest (ClInPc) in the doped OLEDs, namely energy transfer from the host excited state or sequential electron and hole capture by the guest (ClInPc). In energy-transfer processes, the electrons and holes are initially injected into the organic host transport materials, producing either a singlet or triplet exciton and the excitation is then transferred to the guest (ClInPc) by means of a Förster [27] or Dexter [28] process, respectively. In the charge trapping process [29,30], the guest (ClInPc) functions as a recombination center for holes and electrons injected from the ITO electrode through the organic functional layers, and the Al electrode, respectively, leading to the formation of the guest (ClInPc) in an electronically excited state, from which excitation transition to the ground state occurs to give the (NIR) EL. The Förster energy transfer can be easily evaluated from the overlapping of the absorption and emission spectra, and the electron and hole trapping mechanism is most favorable if the highest occupied molecular orbital (HOMO) of the guest is above that of the host, and if the lowest unoccupied molecular orbital (LUMO) is below that of the host [31].

In terms of the results obtained for the ClInPc-doped Alq_3-based OLEDs, as shown in Fig. 3, there was only a small overlap between the PL spectrum of Alq_3 and the B band of the ClInPc, which suggests that Förster energy transfer plays a minor role in these devices [14,30,31]. Fig. 5(a) shows the energy band diagram of the ClInPc-doped Alq_3-based OLEDs. The ClInPc energy levels were extracted from electrochemical measurements in THF. The HOMO and LUMO of ClInPc are −5.05 and −3.50 eV, respectively, just falling within the band gap of the Alq_3; hence, the ClInPc could function as both a hole trap and an electron trap [14,31,32]. The results imply that direct charge trapping seems to be the dominant mechanism in these devices and so it can be proposed that the formation of the excited state occurred directly on ClInPc by trapping holes injected from NPB and electrons injected from Alq_3, and the Alq_3 green emission intensity decreased with increasing dope concentration. Fig. 5(b) shows the current density–voltage characteristics of ClInPc-doped Alq_3-based OLEDs with different ClInPc concentrations in Alq_3. In the case of low dope concentration (10%) the driving voltages of doped devices were higher than those of the undoped devices, which supports the proposal that a direct charge trapping process occurs. When the dope concentration was >10% direct hole injection from NPB into ClInPc and direct electron injection from Alq_3 into ClInPc may lead to lower driving voltages. These results also suggest that the dominant mechanism is direct charge trapping in these ClInPc-doped Alq_3-based OLEDs and therefore, that Förster and Dexter energy transfers play a minor role. Additionally, the NIR OLEDs were stable during operations at these driving voltages.

As polymer based OLEDs are very attractive for large-area and flexible devices because they can be fabricated by processing the active materials from solution at room temperature, devices with the structure: ITO/PVK:ClInPc/BCP/Alq_3/Al were

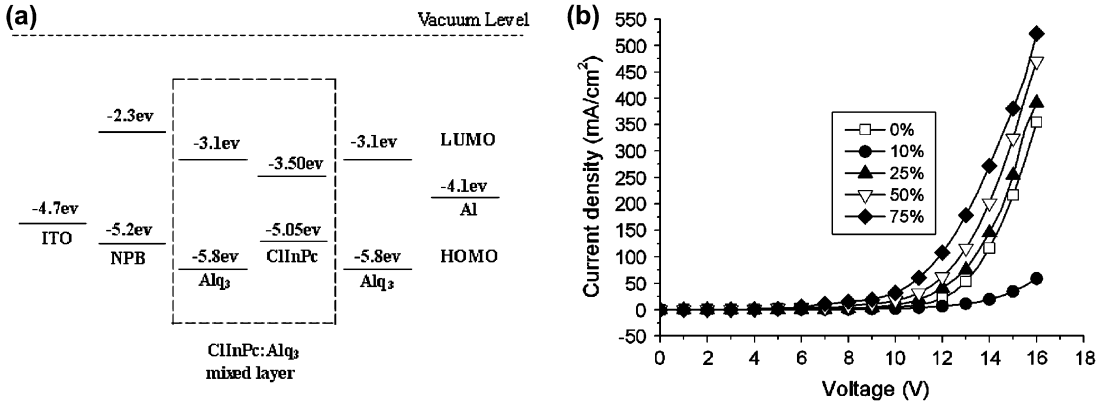

Fig. 5. (a) Schematic description of energy band diagram of ClInPc-doped Alq_3-based OLEDs. (b) The current density–voltage characteristics of ClInPc-doped Alq_3-based OLEDs with different ClInPc concentrations.

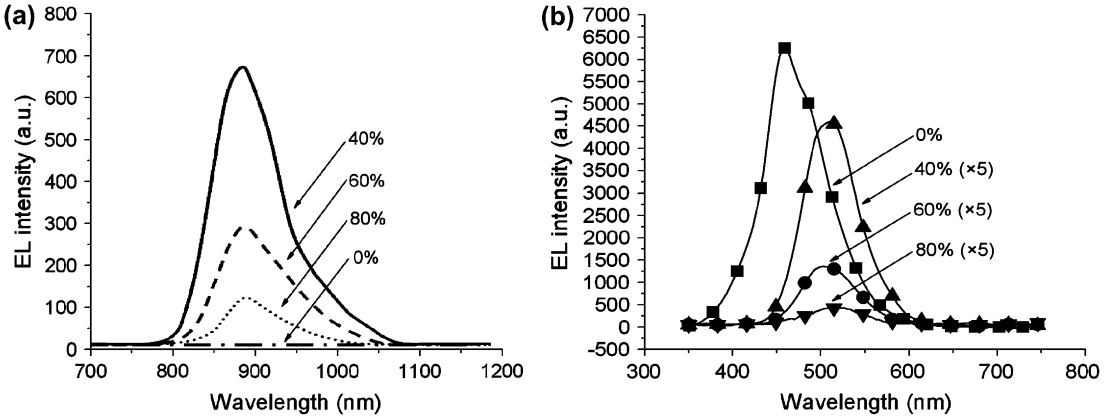

Fig. 6. (a) The NIR EL spectra of devices with the structure of ITO/PVK:ClInPc/BCP/Alq_3/Al with different ClInPc concentrations. (b) The UV–vis EL spectra of devices with the structure of ITO/PVK:ClInPc/BCP/Alq_3/Al with different ClInPc concentrations. The profile of the doped devices has been multiplied by 5.

also fabricated. Fig. 6(a) shows the NIR EL spectra of devices with different concentrations of ClInPc in PVK measured at 10 mA at room temperature. The EL spectra that appeared at about 0.88 μm resembled those of the ClInPc-doped Alq_3-based OLEDs shown in Fig. 4, which implies that the EL originated from the ClInPc and that the shape of the EL spectra should be independent of the host materials. When the concentration of ClInPc was >40%, the intensity of the NIR emission decreased with increasing dope concentration. This finding may be due to fluorescence quenching becoming very prominent at high concentration. The optimum concentration was 40%, which was the same as that in the doped Alq_3-based OLEDs.

Fig. 6(b) shows the UV–vis EL spectra of devices with the structure: ITO/PVK:ClInPc/BCP/Alq_3/Al that comprised different concentrations of ClInPc in PVK at 10 mA at room temperature. The green emission of the doped devices near 510 nm was from Alq_3, whereas the blue emission of the undoped devices near 458 nm came from PVK. The results may be explained as follows. In the undoped devices, hole injection from the PVK HOMO into BCP HOMO was energetically unfavorable due to the large energy difference between the HOMO levels of PVK and BCP (~0.6 eV) and so the 458 nm emission of the undoped devices came from PVK. In the doped devices, there existed an emission of Alq_3 near 510 nm but no emission of PVK near 458 nm which means that efficient energy transfer from PVK to ClInPc existed in these devices. As a hole-transport material, ClInPc enhanced the hole transfer capability of the ClInPc:PVK mixed layer and there was, therefore, emission of Alq_3 near 510 nm, which decreased in intensity with increasing dope concentration because of the recombination of most of the carriers in the ClInPc:PVK mixed layer.

In terms of the electrically exciting process of ClInPc in doped PVK-based OLEDs, an overlap was observed between the PL spectrum of PVK and the B band of the ClInPc (Fig. 3), which indicated that the PVK (host) doped with ClInPc (guest) system may meet the requirements for efficient Förster energy transfer [14,30,31]. Fig. 7(a) shows that the HOMO and LUMO of ClInPc fall within the band gap of the PVK, so the ClInPc could function as both a hole trap and an electron trap [14,31,32]. This shows that charge trapping also plays an important role in these ClInPc-doped PVK-based EL devices. Fig. 7(b) shows the current density–voltage characteristics of ClInPc-doped PVK-based OLEDs with different ClInPc concentrations in PVK. The

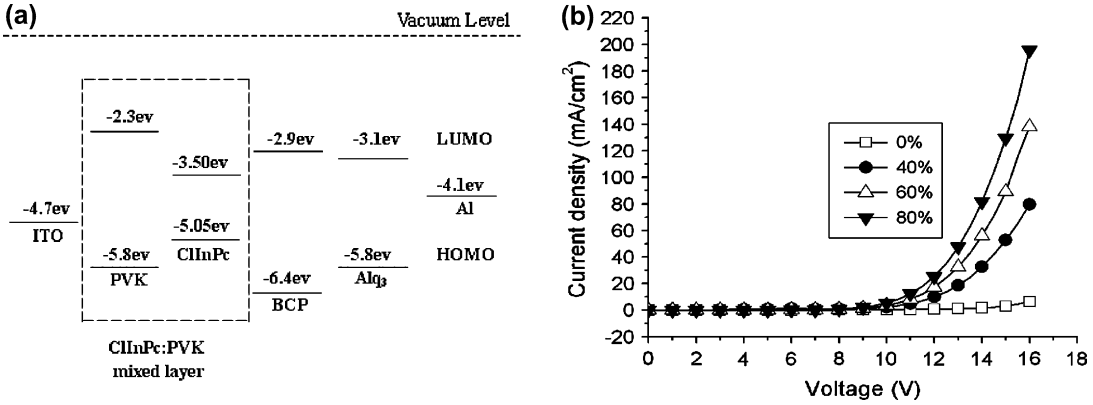

Fig. 7. (a) Schematic description of energy band diagram of ClInPc-doped PVK-based OLEDs. (b) The current density–voltage characteristics of ClInPc-doped PVK-based OLEDs with different ClInPc concentrations.

NIR OLEDs were stable during operation at these driving voltages. The driving voltages decreased with increasing dope concentration which was induced by direct hole injection from ITO into ClInPc and direct electron injection from BCP into ClInPc at high dope concentrations. It seems that both Förster energy transfer and direct charge trapping may play important roles in these doped PVK-based devices.

4. Conclusions

A soluble NIR EL small molecule, chloroindium 1,8(11),15(18),22(25)-tetra-(*p-tert*-butylphenoxy) phthalocyanine, was synthesized successfully and characterized by MS, ^{1}H NMR, elemental analysis, UV–vis and PL. OLEDs with the structures: ITO/ClInPc/Al, ITO/NPB/Alq_3:ClInPc/Alq_3/Al and ITO/PVK:ClInPc/BCP/Alq_3/Al were fabricated. The single-layer device (ITO/ClInPc/Al) did not show any measurable EL due to unbalanced charge injection and unbalanced charge transport. The NIR EL spectra of ClInPc-doped Alq_3-based OLEDs and ClInPc-doped PVK-based OLEDs displayed the characteristic spectrum of ClInPc with a band near 0.88 μm, which coincided with its PL spectrum in the sublimed films. In doped Alq_3-based OLEDs, Förster and Dexter energy transfers play a minor role and the dominant mechanism was direct charge trapping. However, both Förster energy transfer and direct charge trapping may play important roles in doped PVK-based devices.

Acknowledgment

This work was financially supported by the National Natural Science Foundation of China (60307002).

References

[1] Tang CW, Vanslyke SA. Organic electroluminescent diodes. Appl Phys Lett 1987;51:913–5.
[2] Tessler N, Medvedev V, Kazes M, Kan SH, Banin U. Efficient near-infrared polymer nanocrystal light-emitting diodes. Science 2002;295:1506–8.
[3] Slooff LH, Polman A, Cacialli F, Friend RH, Hebbink GA, van Veggel FCJM, et al. Near-infrared electroluminescence of polymer light-emitting diodes doped with a lissamine-sensitized Nd^{3+} complex. Appl Phys Lett 2001;78:2122–4.
[4] Hong ZR, Liang CJ, Li RG, Zang FX, Fan D, Li WL, et al. Infrared and visible emission from organic electroluminescent devices based on praseodymium complex. Appl Phys Lett 2001;79:1942–4.
[5] Kang TK, Harrison BS, Foley TJ, Knefely AS, Boncella JM, Reynolds JR, et al. Near-infrared electroluminescence from lanthanide tetraphenylporphyrin polystyrene blends. Adv Mater 2003;15:1093–7.
[6] Sun RG, Wang YZ, Zheng QB, Zhang HJ, Epstein AJ. 1.54 mm infrared photoluminescence and electroluminescence from an erbium organic compound. Appl Phys Lett 2000;87:7589–91.
[7] Suzukia H. Infrared electroluminescence from an organic ionic dye containing no rare-earth ions. Appl Phys Lett 2002;80:3256–8.
[8] Maya EM, Garcia-Frutos EM, Vazquez P, Torres T. Novel push–pull phthalocyanines as targets for second-order nonlinear applications. J Phys Chem A 2003;107:2110–7.
[9] Crone B, Dodabalapur A, Lin YY, Filas RW, Bao Z, Laduca A, et al. Large-scale complementary integrated circuits based on organic transistors. Nature 2000;403:521–3.
[10] Peumans P, Uchida S, Forrest SR. Efficient bulk heterojunction photovoltaic cells using small-molecular-weight organic thin films. Nature 2003;425:158–62.
[11] Suzette AP, Anne R, Winslow SC. Porphyrin and phthalocyanine anti-scrapie compounds. Science 2000;287:1503–6.
[12] Slyke SAV, Chen CH, Tang CW. Organic electroluminescent devices with improved stability. Appl Phys Lett 1996;69:2160–2.
[13] Fujii A, Ohmori Y, Yoshino K. An organic infrared electroluminescent diode utilizing a phthalocyanine film. IEEE Trans Electron Devices 1997;44:1204–7.
[14] Cheng CH, Fan ZQ, Yu SK, Jiang WH, Wang X, Du GT, et al. 1.1 μm near-infrared electrophosphorescence from organic light-emitting diodes based on copper phthalocyanine. Appl Phys Lett 2006;88:213505.
[15] Sastre A, Gouloumis A, Vázquez P, Torres T, Doan V, Schwartz BJ, et al. Phthalocyanine–azacrown–fullerene multicomponent system synthesis, photoinduced processes and electrochemistry. Org Lett 1999;1:1807–10.
[16] Vacus J, Simon J. Luminescence and anti-aggregative properties of polyoxyethylene-substituted phthalocyanine complexes. Adv Mater 1995;7:797–9.
[17] Ma CY, Tian DL, Hou XK, Chang YC, Cong FD, Yu HF, et al. Synthesis and characterization of several soluble tetraphenoxy-substituted copper and zinc phthalocyanines. Synthesis 2005;5:741–8.
[18] Ma CY, Du GT, Cao Y, Yu SK, Cheng CH, Jiang WH, et al. Synthesis and electrochemistry of a substituted phthalocyaninatozinc. Dyes Pigments 2007;72:267–70.
[19] Snow AW, Jarvis NL. Molecular association and monolayer formation of soluble phthalocyanine compounds. J Am Chem Soc 1984;106:4706–11.
[20] Dodsworth ES, Lever ABP, Seymour P, Leznoff CC. Intramolecular coupling in metal-free binuclear phthalocyanines. J Phys Chem 1985;89:5698–705.
[21] Leznoff CC, Lever ABP. Phthalocyanines: properties and applications, vol. 1. New York: VCH; 1989.
[22] Shirk JS, Pong RGS, Flom SR, Heckmann H, Hanack M. Effect of axial substitution on the optical limiting properties of indium phthalocyanines. J Phys Chem A 2000;104:1438–49.
[23] Chen Y, Hanack M, Blau WJ, Dini D, Liu Y, Lin Y, et al. Soluble axially substituted phthalocyanines: synthesis and nonlinear optical response. J Mater Sci 2006;41:2169–85.
[24] Wang SQ, Gan Q, Zhang YF, Li SY, Xu HJ, Yang GQ. Optical-limiting and photophysical properties of two soluble chloroindium phthalocyanines with α- and β-alkoxyl substituents. ChemPhysChem 2006;7:935–41.
[25] Schouwink P, Schafer AH, Seidel C, Fuchs H. The influence of molecular aggregation on the device properties of organic light emitting diodes. Thin Solid Films 2000;372:163–8.
[26] Caño TD, Parra V, Mendez MLR, Aroca R, Saja JAD. Molecular stacking and emission properties in Langmuir–Blodgett films of two alkyl substituted perylene tetracarboxylic diimides. Org Electron 2004;5:107–14.
[27] Förster T. Intermolecular energy transference and fluorescence. Ann Physik 1948;2:55–75.
[28] Dexter DL. A theory of sensitized luminescence in solids. J Chem Phys 1953;21:836–50.
[29] Suzuki H, Hoshino A. Effects of doping dyes on the electroluminescent characteristics of multilayer organic light-emitting diodes. J Appl Phys 1996;79:8816–22.
[30] Gong X, Lim SH, Ostrowski JC, Moses D, Bardeen CJ, Bazan GC. Phosphorescence from iridium complexes doped into polymer blends. J Appl Phys 2004;95:948–53.
[31] Gong X, Ostrowski JC, Moses D, Bazan GC, Heeger AJ. Electrophosphorescence from a polymer guest–host system with an iridium complex as guest: Förster energy transfer and charge trapping. Adv Funct Mater 2003;13:439–44.
[32] Campbell IH, Smith DL, Tretiak S, Martin RL, Neef CJ, Ferraris JP. Excitation transfer processes in a phosphor-doped poly(*p*-phenylene vinylene) light-emitting diode. Phys Rev B 2002;65:085210.